Available online at www.sciencedirect.com
SCIENCE DIRECT®
Biochemical Pharmacology 68 (2004) 1297–1307
Biochemical Pharmacology
www.elsevier.com/locate/biochempharm

Cyclic antimicrobial peptides based on *Limulus* anti-lipopolysaccharide factor for neutralization of lipopolysaccharide

Jörg Andrä[a], Marta Lamata[b], Guillermo Martinez de Tejada[b], Rainer Bartels[a], Michel H.J. Koch[c], Klaus Brandenburg[a,*]

[a]*Forschungszentrum Borstel, Leibniz-Zentrum für Medizin und Biowissenschaften, Biophysik, Parkallee 10, 23845 Borstel, Germany*
[b]*Dept. de Microbiologia, Universidad de Navarra, Irunlarrea 1, 31008 Pamplona, Spain*
[c]*European Molecular Biology Laboratory c/o DESY, Notkestr. 85, 22603 Hamburg, Germany*

Received 8 April 2004; accepted 26 May 2004

Abstract

Bacterial endotoxin (lipopolysaccharide, LPS) is responsible for the septic shock syndrom. As potential therapeutic agents cyclic cationic antimicrobial peptides of different length, based on the *Limulus* anti-lipopolysaccharide factor (LALF), were synthesized, and their interaction with LPS was characterized physico-chemically and related to results in biological assays. All peptides inhibited the LPS-induced cytokine production in human mononuclear cells and the *Limulus* amebocyte lysate in a concentration-dependent way, with the peptide comprising the complete LPS-binding loop of the LALF (cLALF22) being the most effective. The peptides were neither cytotoxic nor hemolytic, except a slight effect of cLALF22. The peptides were able to displace Ca^{2+} cations from a LPS monolayer, with cLALF22 being again most effective in accordance with results from isothermal titration calorimetry, in which saturation of binding was observed at an equimolar [cLALF22]:[LPS] ratio, and at a ratio 2–2.5 for the other peptides. For cLALF22, zeta (ζ) potential experiments exhibited a complete compensation of the negative charges of LPS, whereas for the other peptides a residual negative potential of −20 to −40 mV was found. X-ray diffraction experiments showed that the mixed unilamellar/cubic inverted aggregate structure of the lipid A part of LPS was converted into a multilamellar one. The gel to liquid crystalline phase transition of the acyl chains of LPS was changed upon cLALF22 binding, leading to a clear fluidization, which was not observed or only to a lesser degree for the other peptides. The affinity of the peptides for LPS led to a reduced binding of lipopolysaccharide-binding protein (LBP) to target membranes and hence to an inhibition of cytokine induction in human mononuclear cells.

Keywords: Antimicrobial peptide; LPS neutralization; Cytokine induction; *Limulus* test; LALF; Tumor-necrosis-factor-α

1. Introduction

Septic shock arises from a cascade of molecular and cellular events following infection by microorganisms, in particular those of Gram-negative origin. Specific cell wall-bound molecules of bacterial cells such as lipopolysaccharide (LPS), which are released into the environment by the attack of the immune system or simply due to cell division, are responsible for this pathogenicity mechanism of the bacteria and are therefore referred to as endotoxins [1]. An initial event in this cascade is the interaction of LPS with serum proteins such as lipopolysaccharide-binding protein (LBP) and with specific receptors and/or binding proteins of immune cells such as CD14 which eventually leads to cell activation [2–4]. The hydrophobic moiety of LPS, lipid A, anchoring the LPS into the outer membrane, constitutes the 'endotoxic principle' of LPS, because it was found that the main biological activities are entirely dependent by this molecular portion [5]. As in other enterobacteriaceae, lipid A from *E. coli* consists of a diglucosamine backbone phosphorylated at positions 1 and 4′ to which six acyl chains are linked at positions 2,3 and 2′,3′. From these considerations it can be assumed that a neutralization of lipid A in particular by cationic agents may be achieved,

Abbreviations: LPS, lipopolysaccharide; FTIR, Fourier-transform infrared spectroscopy; FRET, fluorescence resonance energy transfer spectroscopy; MNC, mononuclear cells; LALF, *Limulus* anti-lipopolysaccharide factor

* Corresponding author. Tel.: +49-4537-188235; fax: +49-4537-188632.
E-mail address: kbranden@fz-borstel.de (K. Brandenburg).

0006-2952/$ – see front matter © 2004 Elsevier Inc. All rights reserved.
doi:10.1016/j.bcp.2004.05.054

which would lead to a protection against LPS-mediated septic shock.

A protein known to inhibit the activation cascade is the *Limulus* anti-lipopolysaccharide factor (LALF) from the horseshoe crab *Limulus polyphemus* [6,7]. LALF-based partial structures containing the LPS-binding domain were found to have a high affinity for endotoxin-binding and -neutralizing, comparable to that of the parent recombinant rLALF (also called endotoxin-neutralizing protein ENP) [8], and to be non-toxic for cultured human monocytes or erythrocytes. This suggests that the rLALF-derived lipid A-binding peptides, in particular in a cyclic conformation, could be promising candidates for use as anti-septic shock agents.

The application and possible development of further derivatives requires the understanding of the physicochemistry of the endotoxin:peptide interaction. We have therefore synthesized a number of these cyclic peptides and have performed a broad biophysical characterization of their interaction with deep rough mutant LPS Re from *Salmonella minnesota* strain R595, which has a well-defined chemical structure, and with the 'endotoxic principle' lipid A. Information was obtained about the changes of the aggregate structure, the mobility of the acyl chains, and the binding epitopes, in particular the negative charges within the lipid A moiety, due to peptide binding. Correlation of these results with data on the cytokine-inhibiting capacity of the peptides clearly establishes that the activity of the peptides is linked to their affinity for LPS, which is in competition to the affinity of LPS for lipopolysaccharide-binding protein. These data allow an understanding of the mechanism of the endotoxin:peptide interaction as prerequisite for the development of even more effective drugs.

2. Materials and methods

2.1. Lipids

Lipopolysaccharide from the deep rough mutant Re *Salmonella minnesota* (R595) was extracted by the phenol/chloroform/petrol ether method [9] from bacteria grown at 37 °C, purified, and lyophilized. Free lipid A was isolated by acetate buffer treatment of LPS R595. After isolation, the resulting lipid A was purified and converted to its triethylamine salt. Results of all the standard assays performed on the purified LPS and lipid A (analysis of the amount of glucosamine, total and organic phosphate, and the distribution of the fatty acid residues) were in good agreement with the chemical properties expected for LPS R595, whose molecular structure has already been solved [1].

2.2. Preparation of endotoxin aggregates

LPS or lipid A was solubilized in the appropriate buffer (lipid concentration 1–10 mM, depending on the applied technique), extensively vortexed, sonicated for 30 min in a water bath, and subjected to several temperature cycles between 20 and 60 °C. Finally, the lipid suspension was incubated at 4 °C for at least 12 h before use.

2.3. Peptides and proteins

Peptides containing the described LPS-binding domain of LALF [8] termed cLALF10, 11, 14, 22 (structures see Fig. 1) were synthesized with an amidated C-terminus by the solid-phase peptide synthesis technique on an automatic peptide synthesizer (model 433 A; Applied Biosystems) on the standard Fmoc-amide resin according to the fastmoc synthesis protocol of the manufacturer. The N-terminal Fmoc-group was removed from the peptide-resin and the peptide was deprotected and cleaved with 90% TFA, 5% anisole, 2% thioanisole, 3% dithiothreitol for 3 h at room temperature. After cleavage the suspension was filtered and the soluble peptides were precipitated with ice-cold diethylether followed by centrifugation and extensive washing with ether. Peptides were purified by RP-HPLC using an Aqua-C18 column (Phenomenex) Elution was done by using a gradient of 0–70% acetonitrile in 0.1% trifluoroacetic acid (TFA). Cyclation via cystein residues was achieved by incubating the peptides in 10% DMSO for 24 h at room temperature. The peptides were then again purified by reversed-phase HPLC to purities above 95%. Purity was determined by laser-desorption-time-of-flight mass spectrometry (MALDI-TOF MS, Bruker). Recombinant *Limulus* anti-LPS-factor, termed endotoxin-neutralizing protein (ENP) was a kind gift of Richard Ridge (Associates of Cape Cod), and lipopolysaccharide-binding protein was from Russ Dedrick (XOMA Co.). LBP was stored at −70 °C as a 1 mg/ml stock solution in 10 mM Hepes, pH 7.5, 150 mM NaCl, 0.002% (v/v) Tween 80, 0.1% F68.

Mouse anti-human LBP-antibody biG42 was purchased from Biometec.

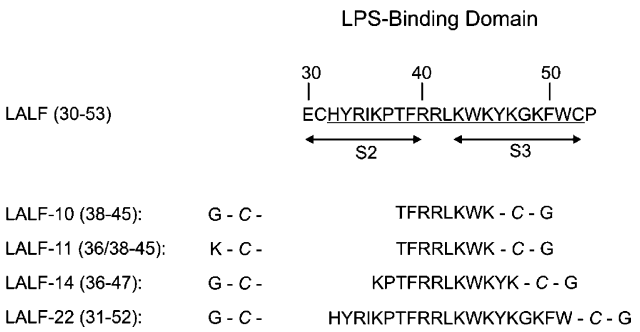

Fig. 1. Amino acid sequences (one-letter code) of the synthetic cyclic peptides cLALF10, cLALF11, cLALF14, and cLALF22 based on the LPS-binding domain of the parent *Limulus* anti-LPS-factor (LALF). S2, S3 = β-strands of the binding domain. The cLALF peptides are shown in linear form and the C residues involved in cyclisation are in italics.

2.4. Determination of endotoxin activity by the chromogenic Limulus test

Endotoxin activity of [LPS]:[peptide] mixtures was determined by a quantitative kinetic assay based on the reactivity of Gram-negative endotoxin with *Limulus* amebocyte lysate (LAL) at 37 °C, using test kits of LAL Coamatic Chromo-LAL K (Chromogenix, Haemochrom) [10]. The standard endotoxin used in this test was from *E. coli* (O55:B5) and 10 endotoxin units (EU/ml) corresponds to 1 ng/ml. In this assay, saturation occurs at 125 EU/ml and the resolution limit is >0.1 EU/ml (maximum value for endotoxin-free water, Aqua B. Braun). The same water was used for the dilution of samples.

2.5. Stimulation of human mononuclear cells by LPS

Mononuclear cells (MNC) were isolated from heparinized blood of healthy donors as described previously [11]. The cells were resuspended in medium (RPMI 1640) and their number was equilibrated at 5×10^6 cells/ml. For stimulation, 200 μl MNC (1×10^6 cells) were transferred into each well of a 96-well culture plate. LPS Re and LPS:cLALF mixtures were preincubated for 30 min at 37 °C, and added to the cultures at 20 μl per well. The cultures were incubated for 4 h at 37 °C under 5% CO_2. Supernatants were collected after centrifugation of the culture plates for 10 min at 400 × *g* and stored at −20 °C until immunological determination of TNFα, carried out in a Sandwich ELISA using a monoclonal antibody against TNF (clone 6b from Intex AG, Switzerland) and was described earlier in detail [11].

2.6. Competitive ELISA

LPS Re (50 μl, 5 μg/ml in phosphate buffered saline; PBS, 140 mM NaCl, 2.7 mM KCl, 8 mM Na_2HPO_4, 2.4 mM KH_2PO_4, pH 7.2) was coated on flexible 96-well ELISA plates (U-form, Falcon) over night at 4 °C under constant shaking. The liquid was removed and the plates were washed extensively with PBS, blocked by incubation with 10% milk powder (low fat) in PBS for 1 h at 37 °C, washed once more with PBS, and incubated with 100 μl of a LBP:peptide mixture at the indicated molar ratios in PBS (LBP concentration 5 μg/ml) overnight at 4 °C under constant shaking. The liquid was removed and the plates were washed extensively with PBS, incubated with an monoclonal anti-LBP antibody (biG42; Biometec, Greifswald, Germany, 1:5000 in 5% milk powder/PBS) for 1 h at 37 °C, washed again, incubated with a horseradish peroxidase-conjugated secondary antibody against mouse IgG (Sigma, 1:10,000 in 5% milk powder/PBS) over night at 4 °C, washed again, and developed with tetramethylbenzidine/H_2O_2. The emerging colour reaction was stopped by adding sulfuric acid and the plates were analyzed in a microtiter plate reader (Rainbow, Tecan, Crailsham, Germany) at 450 nm. Data represent the mean of three independent experiments performed in duplicates. Percent inhibition of LBP binding to LPS was calculated as $\%\text{inh} = [1 - ((I_c - I_0)/(I_{exp} - I_0))] \times 100$ with I_{exp}, ELISA signal of the indicated LBP:peptide mixture; I_c, signal of the respective concentration of LBP; I_0 signal of LPS background.

2.7. Hemolytic activity

Red blood cells (RBCs) were obtained from citrated human blood by centrifugation (1500 × *g*, 10 min), washed three times with isotonic 20 mM phosphate–NaCl buffer (pH 7.4), and suspended in the same buffer at a concentration equivalent to 5% of the normal hematocrit. Forty microliters aliquots of this RBC suspension were added to 0.96 ml of peptide dilutions prepared in the same isotonic phosphate solution, incubated at 37 °C for 30 min and centrifuged (1500 × *g*, 10 min). The supernatants were analyzed spectrophotometrically (absorbance at 543 nm) for hemoglobin and results expressed as percentage released with respect to sonicated controls (100% release) or controls processed without peptides (0% release) [12].

2.8. Cytotoxicity assays

Cytotoxicity was assayed on HeLa cells using the MTT [3-(4,5-dimethylthiazoyl-2-yl)-2,5 diphenyltetrazolium bromide]-PMS (phenazine methosulfate) protocol with modifications [13]. Briefly, cells were grown in Dulbeccos's modified Eagle's medium (DMEM) to a density of 2×10^6 cells/ml and distributed (100 μl or 2×10^5 cells per well) in 96 wells (flat-bottom) polystyrene plates. Plates were incubated for 16 h at 37 °C in 5% CO_2, atmosphere, then supplemented with increasing amounts of peptides (see Section 3) diluted in 2 mM Hepes pH 7.2, and incubation carried on for 20 h under the same conditions, as determined in preliminary experiments. After this time, filter-sterilized MTT and PMS solutions (2 and 0.92 mg/ml, respectively) in Dulbecco's phosphate buffered saline (2.68 mM KCl, 137 mM NaCl, 1.47 mM KH_2PO_4, 8.1 mM Na_2HPO_4, 0.9 mM $CaCl_2 \cdot 2H_2O$, 0.5 mM $MgCl_2$, pH 6.5) were mixed in a 20:1 proportion in the dark, and 25 μl added to each well. After 30 min of incubation, the content of the wells was gently mixed with 100 μl of 40 mM HCl in isopropanol and the absorbance at 550 nm determined in a Titertek Multiscan (Flow Laboratories Inc.) plate reader. Controls were cells incubated without peptide (negative control) or with 10 μl dimethylsulfoxide (positive control). In each case, an aliquot of the cells was taken before MTT-PMS addition, and cell viability examined by the trypan blue exclusion test as described elsewhere [14] with results coincident with the MTT test.

2.9. Fourier-transform infrared spectroscopy (FTIR)

The infrared spectroscopic measurements were performed on an IFS-55 spectrometer (Bruker). Samples, dissolved in 20 mM Hepes buffer, pH 7.0, were placed in a CaF_2 cuvette with a 12.5 μm teflon spacer. Temperature-scans were performed automatically between 10 and 70 °C with a heating-rate of 0.6 °C/min. Every 3 °C, 50 interferograms were accumulated, apodized, Fourier-transformed, and converted to absorbance spectra.

2.10. ^{45}Ca displacement

To investigate the ability of the cLALF peptides to displace divalent Ca^{2+} cations from LPS monolayers, a subphase with 12.5 μM Ca^{2+} doped with radioactive $^{45}Ca^{2+}$ (at a final activity of 250 Bq/ml, Amersham-Buchler) was used. The experiments were performed as described [15] using a LPS Re monolayer (10 nmol/112 cm^2). The peptides were added to the subphase (60 ml) in different concentrations, and the equilibrium β-counting rates were recorded. The relative $^{45}Ca^{2+}$ concentration was calculated from the equation $I_{rel} = (I_{pep} - I_{sub})/(I_{mono} - I_{sub})$, with I_{rel} = relative $^{45}Ca^{2+}$ intensity, I_{sub}, I_{mono}, and I_{pep} the β-intensities of the pure subphase, the activity measured after spreading of the monolayer, and after peptide addition, respectively.

2.11. Zeta potential

Zeta potentials were determined with a Zeta-Sizer 4 (Malvern Instr.) from the electrophoretic mobility by laser-Doppler anemometry at a scattering angle of 90° as described earlier [16]. The zeta potential was calculated according to the Helmholtz–Smoluchovski equation from the mobility of the aggregates in a driving electric field of 19.2 V cm^{-1}. LPS aggregates (0.1 mM) and peptide stock solutions (1–2 mM) were prepared in 10 mM Tris, 2 mM CsCl, pH 7.0, which turned out to give the most reproducible results.

2.12. Isothermal titration calorimetry (ITC)

Microcalorimetric measurements of peptide binding to endotoxins were performed on a MCS isothermal titration calorimeter (Microcal Inc.) at 37 °C as recently described [17]. Endotoxin samples (0.05–0.15 mM)—prepared as described above—were dispensed into the microcalorimetric cell (volume 1.3 ml) and peptide solutions in the concentration range 0.5–5 mM were filled into the syringe compartment (volume 100 μl), each after thorough degassing of the suspensions. After temperature equilibration, the peptides were titrated in 3 μl portions every 5 min into the lipid-containing cell under constant stirring, and the measured heat of interaction after each injection measured by the ITC instrument was plotted versus time. As dilution of the peptides into pure buffer solution gave only negligible heat of dilution, the total heat signal from each experiment was determined as the area under the respective single peaks and plotted versus the [peptide]:[lipid] molar ratio. Since the instrument works in temperature equilibrium at a constant 'current feedback' corresponding to a power of approximately 74 μW, the occurrence of an exothermic reaction leads to a lowering of this current, whereas an endothermic reaction causes an increase. All titration curves were repeated at least twice.

2.13. X-ray diffraction

X-ray diffraction measurements were performed at the European Molecular Biology Laboratory (EMBL) outstation at the Hamburg synchrotron radiation facility HASYLAB using the double-focusing monochromator-mirror camera X33 [18]. Diffraction patterns in the range of the scattering vector $0.07 < s < 1\ nm^{-1}$ ($s = 2 \sin\theta/\lambda$, 2θ scattering angle and λ the wavelength = 0.15 nm) were recorded at 40 °C with exposure times of 2 or 3 min using a linear detector with delay line readout [19]. The s-axis was calibrated with tripalmitate which has a periodicity of 4.06 nm at room temperature. Details of the data acquisition and evaluation system can be found elsewhere [20]. The diffraction patterns were evaluated as described previously [21] assigning the spacing ratios of the main scattering maxima to defined three-dimensional structures. The lamellar and cubic structures are most relevant here. They are characterized by the following features.

(1) Lamellar: the reflections are grouped in equidistant ratios, i.e., 1, 1/2, 1/3, 1/4, etc. of the lamellar repeat distance d_l.
(2) Cubic: the different space groups of these non-lamellar three-dimensional structures differ in the ratio of their spacings. The relation between reciprocal spacing $s_{hkl} = 1/d_{hkl}$ and lattice constant a is

$$s_{hkl} = \left[\frac{(h^2 + k^2 + l^2)}{a}\right]^{1/2}$$

($(h\ k\ l)$ is the Miller indices of the corresponding set of plane).

2.14. Fluorescence resonance energy transfer spectroscopy (FRET)

The ability of the peptides to intercalate into phospholipid liposomes and to inhibit the lipopolysaccharide-binding protein-mediated intercalation of LPS was investigated by FRET as described earlier [11,22]. Briefly, phospholipid liposomes from phosphatidylserine (PS) or from a phospholipid mixture corresponding to the composition of the macrophage membrane [23] were doubly labeled with the fluorescent phospholipid dyes *N*-(7-nitrobenz-2-oxa-1,3-

diazol-4yl)-phosphatidyl ethanolamine (NBD-PE) and *N*-(lissamine rhodamine B sulfonyl)-phosphatidylethanolamine (Rh-PE) (Molecular Probes). Intercalation of unlabeled molecules into the doubly labeled liposomes leads to probe dilution and with that to a lower FRET efficiency: the emission intensity of the donor I_D increases and that of the acceptor I_A decreases (for clarity, only the quotient of the donor and acceptor emission intensity is shown here).

In all experiments, cLALF peptides (100 μl of 100 μM) or mixtures of peptides with LPS (molar ratio 1:1) were added to doubly labelled liposomes (900 μl of 10 μM) at 50 s after equilibration. NBD-PE was excited at 470 nm and the donor and acceptor fluorescence intensities were monitored at 531 and 593 nm, respectively. After 100 s, LBP (5.5 μg) was added and the fluorescence signal I_D/I_A was recorded for 250 s.

3. Results

3.1. Biological activities

In the following, the capacity of the cLALF compounds (chemical structures see Fig. 1) to inhibit the LPS-induced activation of human mononuclear cells (MNC) and the coagulation of the *Limulus* amebocyte lysate as well as the hemolytic activity and cytotoxicity are described. Fig. 2 illustrates that all peptides are able to effectively inhibit the LPS-induced production of tumor-necrosis-factor-α (TNFα) in human MNC. Thus, when added at a [peptide]:[LPS] molar ratio of 15, which corresponds to 9 ng/ml cLALF and 0.5 ng/ml LPS, the cLALF22 peptide reduces the LPS-induced TNFα production to 50% of that measured without peptide, whereas this ratio is >150 for the cLALF10, and intermediate for the other two peptides.

A strong inhibitory effect is similarly observed in the *Limulus* amebocyte lysate coagulation cascade, as exemplified by the behaviour of cLALF10 and cLALF11 in comparison with the parent structure ENP (Fig. 3). Very similar results were found for the other two peptides, i.e., in particular cLALF22 is not more efficient than the other compounds (data not shown).

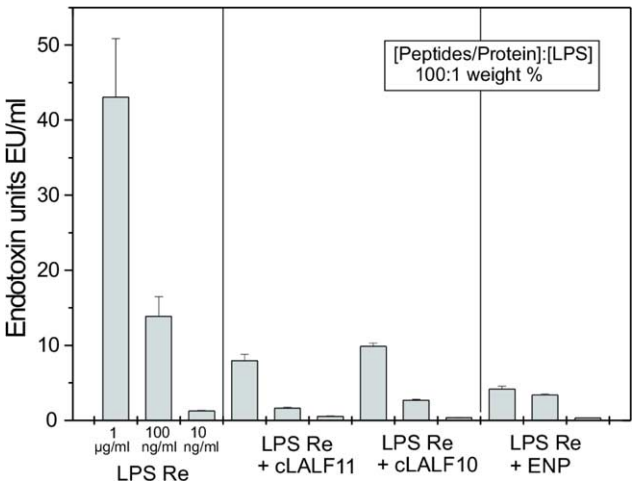

Fig. 3. Inhibition of the LPS-induced reaction in the chromogenic *Limulus* amebocyte lysate assay by cLALF10 and cLALF11 as compared to recombinant LALF (endotoxin-neutralizing protein, ENP). LPS was added at three different concentrations (left section) and the respective reactions in the presence of the peptides and the protein are shown in the middle and right columns.

An important prerequisite for the applicability as antiseptic agent is that it is devoid of cell damaging effects when used in therapeutic concentrations. The test on the haemolytic activity, i.e., the lysis of RBC's due to membrane alterations, revealed only very slight activity for the compounds cLALF10, 11, and 14, but significantly larger effects for cLALF22 (Fig. 4). Note, however, that the peptide concentrations applied here are much larger than those used in the cytokine inhibition test shown in Fig. 2 (maximum concentration <1 μg/ml).

Tests of the cytotoxicity of the peptides on the human HeLa cell line revealed no decrease of the viability of the cells after 16 h of incubation with the peptides up to concentrations of 200 μg/ml (data not shown).

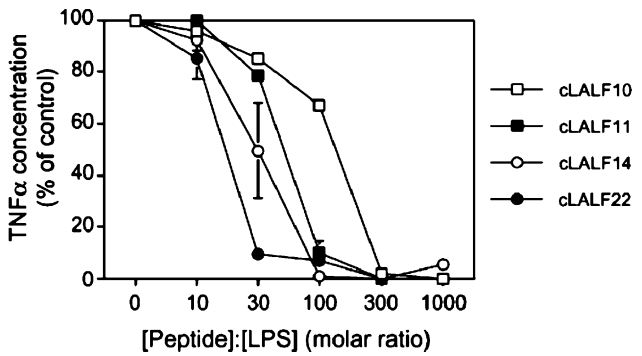

Fig. 2. Inhibition of the LPS-induced production of tumor-necrosis-factor-α (TNFα) by the four cyclic cLALF peptides in a typical experiment ([LPS] = 0.5 ng/ml). The data were confirmed in two further series of experiments. The mean and the standard deviation are based on the data from the determination of TNFα in duplicate at two different dilutions.

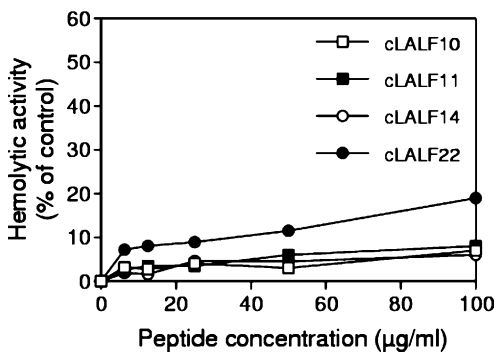

Fig. 4. Hemolytic activity of the four peptides presented as percent of lysis of red blood cells (erythocytes) in dependence on peptide concentration measured spectrophotometrically after addition of the indicated final concentrations of each cLALF peptide. Percentages are calculated relative to a reference cell containing sonicated red blood cells (100% release).

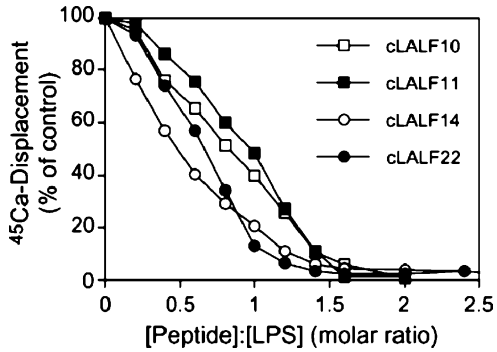

Fig. 5. Displacement of ^{45}Ca from a LPS monolayer measured at different peptide:LPS molar ratios. The β-radiation of ^{45}Ca was measured directly above the subphase with a gas proportional counter.

3.2. Physico-chemical characterization

Various physical techniques were applied to characterize the interaction of LPS, in some cases also of lipid A as endotoxic principle, with the peptides.

The ability of the cLALF peptides to displace $^{45}Ca^{2+}$ cations bound to the backbone of an LPS monolayer is shown in Fig. 5, where cLALF22 proved to be most effective, since an equimolar [cLALF22]:[LPS] ratio is sufficient to release nearly all Ca^{2+} cations. For cLALF14 similar results were obtained, but for cLALF10 and 11 much higher amounts of peptide are required to displace all cations. Summarized, these results suggest that all peptides bind to the negatively charged groups of LPS, essentially the lipid A phosphates and the carboxylates within the 2-keto-3-octonate (Kdo) moiety of LPS.

A more detailed analysis of the binding characteristic was obtained from the electrophoretic mobility of LPS aggregates in the presence of different amounts of peptides in a zeta sizer. The zeta (ξ) potential, a measure of the accessible surface charges, is plotted versus the [peptide]:[LPS] ratio in Fig. 6. Here, the peptide cLALF11 has the lowest capacity ($\xi < -30$ mV) to neutralize the surface charges. Only incomplete compensation of the LPS surface

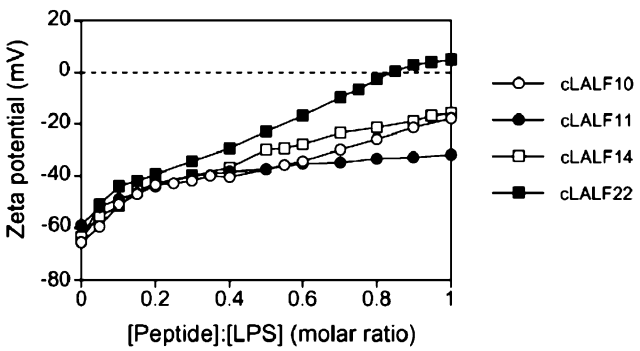

Fig. 6. Zeta potential of LPS aggregates in dependence on different peptide:LPS molar ratios as determined by the electrophoretic mobility by laser-Doppler anemometry.

charges takes place for cLALF10 and 14, even though, for example, cLALF14 bears seven positive charges (including the N-terminus, see Fig. 1). In contrast, cLALF22 even overcompensates the negative surface charges of LPS leading to $\xi > 0$ mV.

Isothermal titration calorimetry is the method of choice to determine the enthalpy change caused by the peptide:LPS binding and its stoichiometry. In Fig. 7, the results are presented for the cLALF10 and cLALF22:LPS systems. It can be deduced from the figure that (i) the negative enthalpy changes ΔH_c after each titration step indicate exothermic reactions; and (ii) while a molar ratio higher than 2 is needed to saturate the binding of cLALF10 to LPS, an equivalent effect is achieved when using cLALF 22 at a peptide:LPS molar ratio of approximately 1. Values for cLALF10 are similar to those for cLALF11 and 14 (data not shown). The maximum enthalpy changes ΔH_c of the peptide binding to LPS indicate relatively low values of −15 kJ/mol for cLALF10 and 11, intermediate values for cLALF14 (approximately −30 kJ/mol, data not shown), and high values for the cLALF22:LPS interaction (−70 kJ/mol, Fig. 7B).

The results of the analysis of the gel to liquid crystalline $\beta \leftrightarrow \alpha$ phase behaviour of the acyl chains of LPS carried out by FTIR in the presence of various peptides is presented in Fig. 8 as plot of the peak position of the symmetric stretching vibrations of the methylene groups versus temperature. For cLALF10 and 11, the phase transition temperature T_c around 32 °C remains nearly unchanged, and the slight increase in the wavenumbers in particular in the liquid crystalline phase indicates a fluidization. The influence of cLALF14 and 22 on the phase transition behaviour are opposite: with cLALF14 the wavenumbers decrease especially in the gel phase which is typical of a rigidification, whereas cLALF22 causes an increase characteristic of a fluidization. Therefore, the action of the peptides on the hydrophobic moiety of LPS is different for each individual peptide.

The kind of aggregate structure of the lipid A part of LPS, which is known to be essential for the expression of biological activity [24,25], was determined by small-angle synchrotron radiation X-ray diffraction. The diffraction patterns for pure lipid A and in the presence of the peptides ([lipid A]:[peptides] 3:1 molar) prove the existence of a mixed unilamellar/non-lamellar cubic structure for pure lipid A (Fig. 9A) and of multilamellar structures for the mixtures (Fig. 9B), as deduced from the spacings at equidistant ratios. The diffraction pattern of the lipid A:cLALF11 complex exhibits two or even three superimposed multilamellar structures with different periodicities. Thus, while the smallest one ($d_{11} = 5.00$ nm) is similar to that for lipid A assembly in the presence of Mg^{2+} [26], the highest values ($d_{12} = 5.90$ nm, $d_{13} = 6.62$ nm) correspond to the lipid A + peptide lamellar stack. For the cLALF14:lipid A complex, two periodicities between 6.22 and 5.75 nm (giving one main reflection at 5.95 nm in the

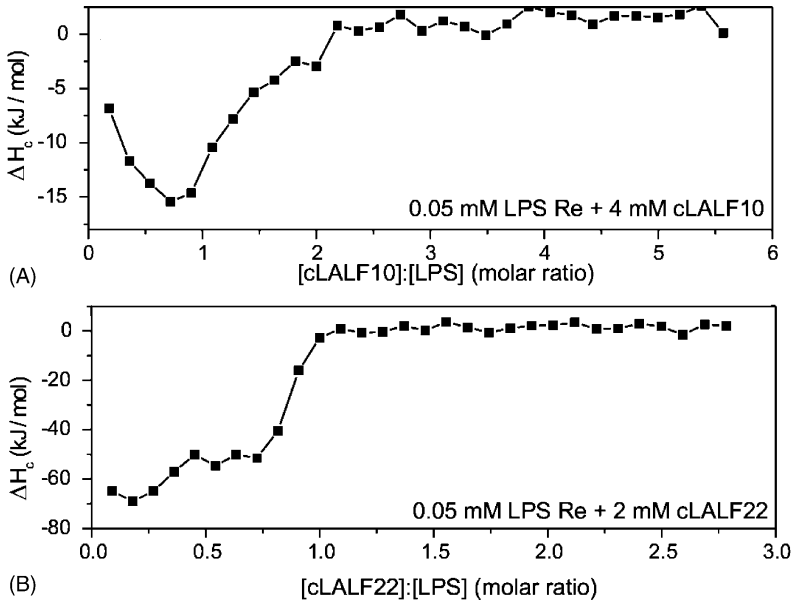

Fig. 7. Enthalpy change ΔH_c of the peptide:LPS binding vs. the peptide:LPS molar ratio as determined by isothermal titration calorimetry. The peptides were titrated by addition of 3 μl portions every 5 min to the LPS suspension until reaching the indicated final concentration.

figure) are observed, deduced from the second- and third-order reflections. For lipid A in the presence of cLALF10, only one lamellar periodicity ($d_l = 5.21$ nm) is observed, but no elongated stacks. In contrast, the lamellar spacing of the lipid A:cLALF22 complex (6.76 nm) indicates that a significantly larger space between neighbouring bilayers is required for peptide insertion into the lipid A aggregate.

3.3. Intercalation into phospholipid membranes

FRET was applied to monitor a possible intercalation of the peptides alone or in the presence of LPS as well as LBP into phospholipid target structures, liposomes from phosphatidylserine or those corresponding to the composition of the macrophage membrane. The results show that all peptides, added after 50 s to PS liposomes, are able to

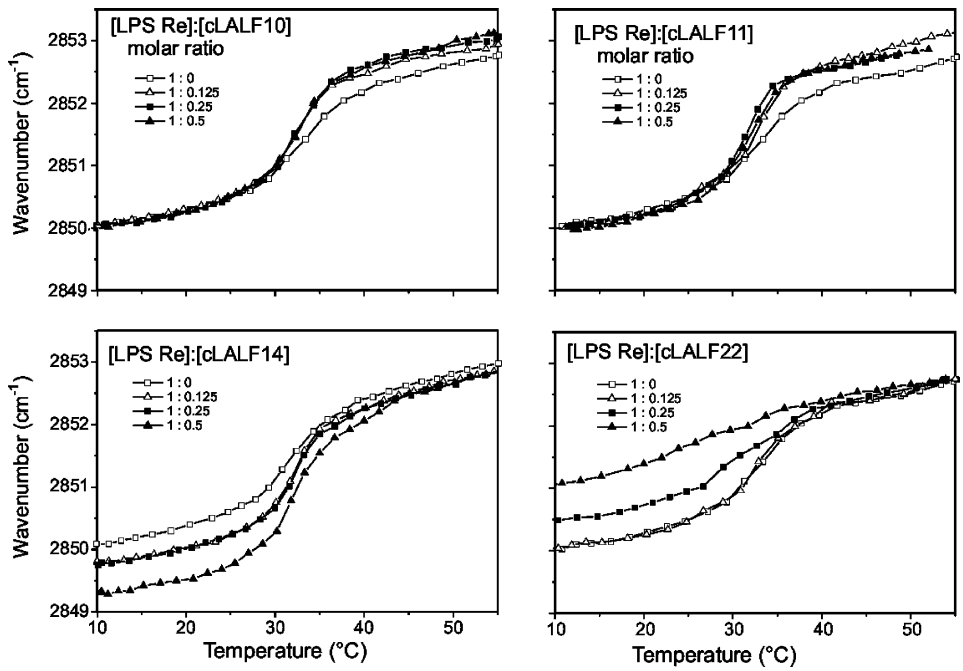

Fig. 8. Gel to liquid crystalline phase transition of the acyl chains of LPS in the presence of different peptide concentrations as determined by FTIR for each of the four peptides. For this, the peak position of the symmetric stretching vibration of the methylene groups $\nu_s(CH_2)$ is plotted vs. the temperature. In the gel phase, the peak position of $\nu_s(CH_2)$ is located around 2850 cm^{-1}, in the liquid crystalline phase around 2852–2853 cm^{-1}.

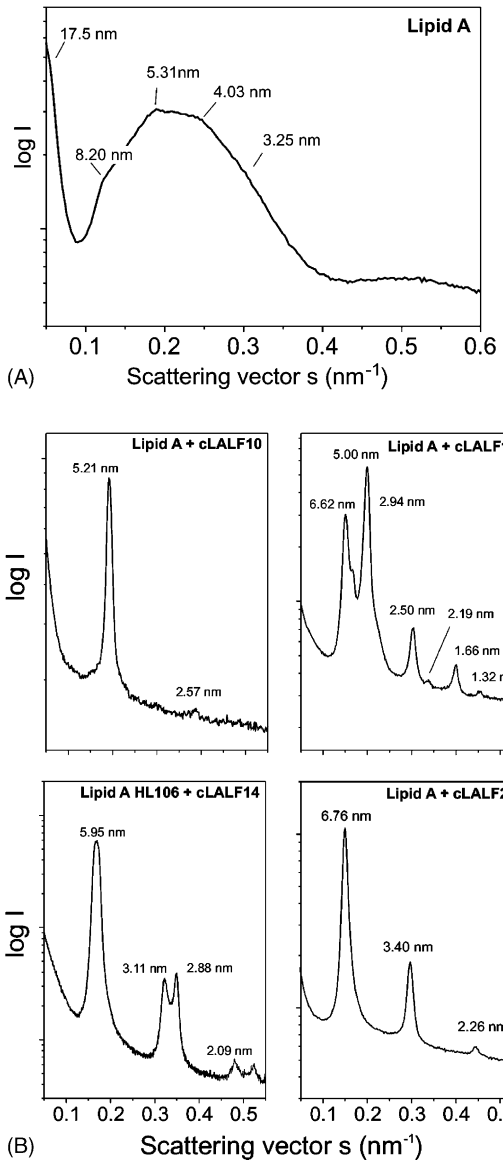

Fig. 9. Small-angle X-ray diffraction patterns of free lipid A from *Salmonella minnesota* deep rough mutant LPS (A) and in the presence of the four peptides at a 3:1 [lipid A]:[peptide] molar ratio (B). The logarithm of the scattering intensity log $I(s)$ is plotted vs. the scattering vector s ($1/d$, d is the spacing ratio).

intercalate into the liposomes, taken from an increase in the FRET signal (Fig. 10, solid line). The subsequent addition of LBP at 100 s leads to another increase, which is strong for cLALF10, less for cLALF11, and much less or even absent for cLALF14 and cLALF22. This can be interpreted, that the latter peptides inhibit LBP to intercalate itself into the target membrane. When the peptides and LPS are added simultaneously after 50 s, a similar increase of the FRET signal is observed as without LPS (Fig. 10, dotted line). However, the addition of LBP at 100 s leads to a strong intensity increase for cLALF10 and cLALF11, but only to a minor increase for cLALF14 and nearly no increase for cLALF22. This means that in particular cLALF22 is able to block the LBP-mediated LPS incorporation. Similar results were found for phospholipid liposomes corresponding the composition of the macrophage membrane, except that the amplidudes of the signals were lower (data not shown).

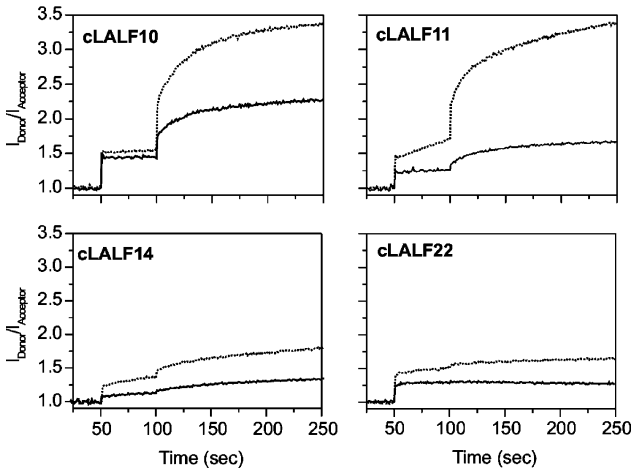

Fig. 10. Change of the FRET signal ($I_{donor}/I_{acceptor}$) due to intercalation into phospatidylserine liposomes after addition of cLALF peptides (solid line) or cLALF-peptides + LPS Re (dashed line) at 50 s and subsequent addition of LBP at 100 s. The final concentration of all compounds was 10^{-5} M.

3.4. LALF peptides binding affinity to LPS

The affinity of the cLALF peptides for LPS Re in terms of LPS:LBP affinity was estimated by a competitive ELISA. Peptides and LBP were preincubated together and given into LPS-coated microtiter plates. The amount of LPS-bound LBP was then determined using a specific anti-LBP antibody. At a [peptide]:[LBP] 100:1 molar ratio, binding of LBP to LPS was prevented by cLALF22 (20% residual LBP binding), but to a much lesser extent by cLALF14 (40% LBP binding) and cLALF10 and cLALF11 (80% LBP binding).

These data allow the conclusion that at sufficiently high peptide concentrations the LBP-binding can be inhibited significantly in particular by cLALF22.

4. Discussion

Synthetic peptides based on the sequence of endotoxin-binding proteins like the LALF protein [8] and also on the bactericidal/permeability increasing protein (BPI) or the lipopolysaccharide-binding protein [27] were investigated by various groups. It was shown that some of these compounds are in principle suitable for application in anti-sepsis research, in particular as they have a sufficiently long half-life in serum [8].

We have synthesized cyclic partial structures of the LALF endotoxin-neutralizing protein, cLALF10, 11, 14 and 22, from the LPS-binding domain (strands S2 and S3,

see Fig. 1), and have subjected them to biological and physico-chemical test systems to characterize their endotoxin-neutralizing capacity and their mode of interaction with LPS. All peptides block the LPS-induced cytokine induction (Fig. 2) and coagulation of the *Limulus* amebocyte lysate (Fig. 3). At the same time, they exhibit only a marginal haemolytic activity, except for cLALF22 (Fig. 4), and no detectable cytotoxicity. The reduction in biological activity is correlated with binding of the peptides to the negatively charged groups of the LPS aggregates, which expresses itself in a displacement of Ca^{2+} cations from LPS monolayers (Fig. 5) and a decrease of the accessible surface charges, as measured by the zeta potential of LPS (Fig. 6). The LPS:peptide binding reaction is essentially exothermic (Fig. 7) suggesting a predominantly electrostatic nature of the binding, whereby the positive charges of the peptides are assumed to bind to the phosphates and carboxylates of LPS.

All peptides convert the unilamellar/cubic structure (Fig 9A) of lipid A into a multilamellar one (Fig. 9B) with variations in the periodicity d_l. The peptides cLALF11 and cLALF22 cause a significant increase in d_l. Since this value comprises the bilayer thickness plus the water layer between adjacent bilayers, one possibility is that these two peptides protrude from the lipid A backbone much more than the other two peptides. However, also other consequences of peptide binding such as different hydration states of the lipid A backbones could hold true.

A comparison of the peptides indicates that the cLALF22 is the most active in inhibiting the cytokine production (Fig. 2). However, this difference is not expressed in the *Limulus* test (data not shown). This observation should be seen in the light of the fact that the latter assay does not necessarily reflect the endotoxicity of LPS, since inactive compounds such as tetra- and pentaacyl lipid A also exhibit high *Limulus* activity [25]. It has been shown that the binding epitopes in the *Limulus* assay is the diglucosamine-4′-phosphate region in the lipid A moiety of LPS [28]. Therefore, from the above results it can be assumed that all four cLALF peptides block the diglucosamine-4′-phosphate molecular group or at least a significant part of this group.

Concomitantly with the reduction in bioactivity, peptide binding results in a displacement of $^{45}Ca^{2+}$ from a LPS monolayer, cLALF22 being again the most effective peptide (Fig. 5). This is equally valid for the compensation of the accessible surface charges of LPS, and thus only this peptide neutralizes the negative charges of LPS completely. On the contrary, for the other peptides still a negative potential of −20 to −40 mV is observed at the point of binding saturation (Fig. 6). The [cLALF]:[LPS] binding stoichiometry is in accordance with these data. For cLALF10, cLALF11, and cLALF14 a value of 2–2.5 is found (Fig. 7A). In contrast, for cLALF22 the binding is saturated at an equimolar ratio (Fig. 7B). Concomitantly, there is an dramatic enhancement of the maximum enthalpy change ΔH_c of the cLALF22 binding to LPS with values around −60 to −70 kJ/mol as compared to −15 to −30 kJ/mol for the other peptides (Fig. 7). This observation is indicative of a much stronger electrostatic interaction of the positive charges of cLALF22 with the negatively charged groups of LPS. Furthermore, only cLALF22 causes a significant fluidization of the lipid A acyl chains (Fig. 8), which is much less pronounced for cLALF10 and 11 and in the case of cLALF14, even reversed indicating a rigidification.

Based on these data it can be hypothesized that the peptides adopt different conformations when interacting with LPS aggregates. Thus, although the number of positive charges of cLALF10, cLALF11, or cLALF14 ($n = 5, 6$ and 7, respectively) should be sufficient to neutralize the four negative charges of LPS, the folding of these peptides does not seem to be suitable for charge compensation in contrast to that of cLALF22 (bearing nine positive charges). In this respect, the behaviour of cLALF22 corresponds to that of the parent ENP.

To correctly interpret the inhibition of the endotoxic effects by the peptides (Figs. 2 and 3), it must be taken into account that the initial events in the LPS-induced cell activation consists of an interaction of serum- and membrane-proteins such as lipopolysaccharide-binding protein and CD14 with LPS aggregates [29,30]. It was proposed previously that soluble LBP disaggregates the LPS polymers and transports probably LPS-monomers to membrane-bound CD14 [31,32], which then in a further step leads to the conformational change of transmembrane proteins such as the Toll-like receptors [33] or the K^+-channel MaxiK [34] with subsequent cell activation. It is believed that once it is associated with the cell membrane, the lipid A moiety of LPS, which for enterobacterial endotoxins has a conical geometrical shape, induces this conformational change due to sterical stress at the site of a signalling protein. It was indeed found that lipid A aggregates with a cylindrical shape (tetra- and pentaacyl lipid A) are unable to induce this change and do not activate the cells [25].

It should be emphasized, that the first steps in this cascade, i.e., the binding of LPS and its transport to CD14 are of hypothetical nature and indeed unlikely to occur, because of the very high affinity of LBP to LPS [35]. LBP has been shown to bind preferentially to negatively charged lipids [36], and in the case of LPS binding results in a higher aggregation rather than to a disaggregation ([37] and own unpublished results).

It should be noted that a membrane-bound form of LBP exists [37,38] This molecule may well be involved in the incorporation of external LPS aggregates into the cell membrane of mononuclear cells, which in turn seems to be an essential step in cell activation. In such a scenario, soluble LBP would scavenge LPS in the serum thus leading to a decrease in its immunostimulatory activity, whereas binding of LPS to the membrane form would lead to

activation. This hypothesis would explain the observation that LBP is a protective agent at high concentrations in the acute phase serum and an activating agent at very low concentrations [39].

Irrespectively of these detailed mechanisms, from the competition assay it becomes evident that the binding-sites of the peptides in the LPS molecules can also be occupied by LBP. Thus, LBP can displace the peptides in the order cLALF10 and 11 < for cLALF14, and ≪ for cLALF22. Hence, at a sufficiently high concentration of cLALF22 much lower amounts of LBP would be able to react with LPS, leading to a strong reduction of cell activation. These data are in excellent accordance with the data from the FRET assay indicating a high intercalation for LBP into phospholipid liposomes in the presence of cLALF10 and cLALF11, but not for cLALF14 and cLALF22 (Fig. 10). This statement is valid in the absence as well as presence of LPS. This means that beside a binding of the peptides to LPS, a necessary condition for inhibition of cell activation is the reduction of an intercalation of LBP into immunocompetent cell membranes, which corresponds to the scenario of cell activation as described above. The parent structure of the LALF peptides, endotoxin-neutralizing protein ENP, has recently been characterized biophysically [40]. Inhibition of the biological activity of LPS, which for ENP occurred already at a molar ratio [ENP]:[LPS] = 2, was accompanied by a neutralization of the negative charges of LPS at a molar ratio of [ENP]:[LPS] = 0.4; at higher ratios, there is an overcompensation of the charges as found here for cLALF22. Also ENP provokes the formation of a multilamellar aggregate structure of lipid A with d_1 =5.10–5.30 nm corresponding to the periodicity of pure lipid A and with d_1 = 7.80–8.20 nm to a mixed ENP:lipid A multilamellar periodicity. However, the action of cLALF22 on LPS differs insofar as it provokes a fluidization of the LPS acyl chains (Fig. 8) in contrast to the rigidifying action of ENP.

One possible explanation of the significantly higher inhibitory activity of ENP as compared to the cyclic derivatives may lie in the fact that similarly to LBP ENP has been described as an endotoxin-transport protein. As found here for the cLALF peptides, it has been shown by FRET that ENP intercalates by itself into target cell membranes. Furthermore, it mediates the incorporation of LPS. Thus, in the target cell membrane ENP may interact with LPS and may lead to a change of the lipid A moiety from conical to cylindrical, thus inhibiting cell activation.

The above results show that the cyclic LALF peptides may be good candidates for use in anti-septic shock therapy. However, since LPS-binding peptides and proteins may rapidly be cleared from the bloodstream thereby becoming ineffective, the next obvious step before clinical application will be the evaluation of the therapeutical potential of the peptides by the application of an animal model similar to that used by Vallespi et al. [41]. These authors used an experimental animal model of Gram-negative sepsis to study the in vivo antiseptic activity of a cyclic LALF-derived peptide, which corresponds to the present cLALF22 except for two amino acid residues. They analysed the pattern of cytokine gene expression in the spleen and liver in peptide- and LPS-treated mice and found an abrogation of a systemic TNFα response, reduced organ damage and increased survival of infected mice.

In future studies, we shall investigate the therapeutical potential of cLALF-based derivatives as anti-septic shock agents. Today's possibilities of large scale production of peptides allowing to scan a wide range of structural variations offers a promising approach for the development of effective therapeutic agents.

Acknowledgments

We are indebted to G. von Busse, U. Diemer, C. Hamann, and K. Stephan for technical assistance in the IR spectroscopic, LAL, FRET, and TNFα measurements, respectively. This work has been carried out with financial support from the Commission of the European Communities, specific RTD programme ''Quality of Life and Management of Living Resources'', ''QLK-CT-2002-01001'', 'Antimicrobial endotoxin neutralizing peptides to combat infectious diseases'.

References

[1] Rietschel ET, Kirikae T, Loppnow H, Zabel P, Ulmer J, Brade H, et al. Molecular aspects of the chemistry and biology of endotoxin. In: Sies H, Flohé L, Zimmer G, editors. Molecular aspects of inflammation. Berlin: Springer-Verlag; 1991. p. 207–31.

[2] Tapping RI, Tobias PS. Cellular binding of soluble CD14 requires lipopolysaccharide (LPS) and LPS-binding protein. J Biol Chem 1997;272:23157–64.

[3] Heumann D, Glauser MP, Calandra T. Molecular basis of host-pathogen interaction in septic shock. Curr Opin Microbiol 1998;1:49–55.

[4] Alexander C, Rietschel ET. Bacterial lipopolysaccharides and innate immunity. J Endotoxin Res 2001;7:167–202.

[5] Zähringer U, Lindner B, Rietschel ET. Chemical structure of lipid A. Recent advances in structrural analysis of a biologically active molecules. In: Brade H, Opal SM, Vogel SN, Morrison DC, editors. Endotoxin in health and disease. New York: Marcel Dekker; 1999. p. 93–114.

[6] Alpert G, Baldwin G, Thompson C, Wainwright N, Novitsky TJ, Gillis Z, et al. *Limulus* antilipopolysaccharide factor protects rabbits from meningococcal endotoxin shock. J Infect Dis 1992;165:494–500.

[7] Hoess A, Watson S, Siber GR, Liddington R. Crystal structure of an endotoxin-neutralizing protein from the horseshoe crab, *Limulus* anti-LPS factor, at 1.5 A resolution. EMBO J 1993;12:3351–6.

[8] Ried C, Wahl C, Miethke T, Wellnhofer G, Landgraf C, Schneider-Mergener J, et al. High affinity endotoxin-binding and neutralizing peptides based on the crystal structure of recombinant *Limulus* anti-lipopolysaccharide factor. J Biol Chem 1996;271:28120–7.

[9] Galanos C, Lüderitz O, Westphal O. A new method for the extraction of R lipopolysaccharides. Eur J Biochem 1969;9:245–9.

[10] Friberger P, Sörskog L, Nilsson K, Knös M. The use of a quantitative assay in endotoxin testing. In: Watson SW, Levin J, Novitzky TJ, editors. Detection of bacterial endotoxin with the *Limulus* amebocyte lysate test. New York: A. Liss; 1987. p. 149–69.
[11] Jürgens G, Müller M, Koch MHJ, Brandenburg K. Interaction of hemoglobin with enterobacterial lipopolysaccharide and lipid A: physicochemical characterization and biological activity. Eur J Biochem 2001;268:4233–42.
[12] Ohtani Y, Irie T, Uekama U, Fukunaga K, Pitha U. Differential effects of alpha-, beta- and gamma-cyclodextrins on human erythrocytes. Eur J Biochem 1989;186:17–22.
[13] Mosmann T. Rapid colorimetric assay for cellular growth and survival: application to proliferation and cytotoxicity assays. J Immunol Methods 1983;65:55–63.
[14] Hudson L, Hay FC. Practical immunology. Oxford: Blackwell Publishers; 1976.
[15] Gutsmann T, Hagge SO, Larrick JW, Seydel U, Wiese A. Interaction of CAP18-derived peptides with membranes made from endotoxins or phospholipids. Biophys J 2001;80:2935–45.
[16] Brandenburg K, Garidel P, Andrä J, Jürgens G, Müller M, Blume A, et al. Cross-linked hemoglobin converts endotoxically inactive pentaacyl endotoxins into a physiologically active conformation. J Biol Chem 2003;278:47660–9.
[17] Brandenburg K, Moriyon I, Arraiza MD, Lehwark-Yvetot G, Koch MHJ, Seydel U. Biophysical investigations into the interaction of lipopolysaccharide with polymyxins. Thermochim Acta 2002;382:189–98.
[18] Koch MHJ, Bordas J. X-ray diffraction and scattering on disordered systems using synchrotron radiation. Nucl Instrum Methods 1983;208:461–9.
[19] Gabriel A. Position-sensitive X-ray detector. Rev Sci Instrum 1977;48:1303–5.
[20] Boulin C, Kempf R, Koch MHJ, McLaughlin SM. Data appraisal, evaluation and display for synchrotron radiation experiments: hardware and software. Nucl Instrum Methods 1986;A249:399–407.
[21] Brandenburg K, Funari SS, Koch MHJ, Seydel U. Investigation into the acyl chain packing of endotoxins and phospholipids under near physiological conditions by WAXS and FTIR spectroscopy. J Struct Biol 1999;128:175–86.
[22] Gutsmann T, Schromm AB, Koch MHJ, Kusumoto S, Fukase K, Oikawa M, et al. Lipopolysaccharide-binding protein-mediated interaction of lipid A from different origin with phospholipid membranes. Phys Chem Chem Phys 2000;2:4521–8.
[23] Kröner EE, Peskar BA, Fischer H, Ferber E. Control of arachidonic acid accumulation in bone marrow-derived macrophages by acyltransferases. J Biol Chem 1981;256:3690–7.
[24] Schromm AB, Brandenburg K, Loppnow H, Zähringer U, Rietschel ET, Carroll SF, et al. The charge of endotoxin molecules influences their conformation and interleukin-6 inducing capacity. J Immunol 1998;61:5464–71.
[25] Schromm AB, Brandenburg K, Loppnow H, Moran AP, Koch MHJ, Rietschel ETh, et al. Biological activities of lipopolysaccharides are determined by the shape of their lipid A portion. Eur J Biochem 2000;267:2008–13.
[26] Brandenburg K, Koch MHJ, Seydel U. Phase diagram of lipid A from *Salmonella minnesota* and *Escherichia coli* rough mutant lipopolysaccharide. J Struct Biol 1990;105:11–21.
[27] Dankesreiter S, Hoess A, Schneider-Mergener J, Wagner H, Mietke T. Synthetic endotoxin-binding peptides block endotoxin-triggered TNF-α production by macrophages in vitro and in vivo and prevent endotoxin-mediated toxic shock. J Immunol 2000;164:4804–11.
[28] Brandenburg K, Jürgens G, Andrä J, Lindner B, Koch MHJ, Blume A, et al. Biophysical characterization of the interaction of high-density lipoprotein (HDL) with endotoxins. Eur J Biochem 2002;269:5972–81.
[29] Tobias PS, Ulevitch RJ. Lipopolysaccharide binding protein and CD14 in LPS dependent macrophage activation. Immunobiology 1993;187:227–32.
[30] Tapping RI, Gegner JA, Kravchenko VV, Tobias PS. Roles for LBP and soluble CD14 in cellular uptake of LPS. Prog Clin Biol Res 1998;397:73–8.
[31] Mathison JC, Tobias PS, Wolfson E, Ulevitch RJ. Plasma lipopolysaccharide (LPS)-binding protein: a key component in macrophage recognition of Gram-negative LPS. J Immunol 1992;149:200–6.
[32] Kirkland TN, Finley F, Leturcq D, Moriarty A, Lee J-D, Ulevitch RJ, et al. Analysis of lipopolysaccharide binding by CD14. J Biol Chem 1993;268:24818–23.
[33] Chow JC, Young DW, Golenbock DT, Christ WJ, Gusovsky F. Toll-like receptor-4 mediates lipopolysaccharide-induced signal transduction. J Biol Chem 1999;274:10689–92.
[34] Blunck R, Scheel O, Müller M, Brandenburg K, Seitzer U, Seydel U. New insights into endotoxin-induced activation of macrophages: involvement of a K^+ channel in transmembrane signaling. J Immunol 2001;166:1009–15.
[35] Tobias PS, Soldau K, Ulevitch RJ. Identification of a lipid A binding site in the acute phase reactant lipopolysaccharide binding protein. J Biol Chem 1989;264:10867–71.
[36] Schromm AB, Brandenburg K, Rietschel ETh, Flad H-D, Carroll SF, Seydel U. Lipopolysaccharide binding protein (LBP) mediates CD14-independent intercalation of lipopolysaccharide into phospholipid membranes. FEBS Lett 1996;399:267–71.
[37] Gutsmann T, Müller M, Carroll SF, MacKenzie RC, Wiese A, Seydel U. Dual role of lipopolysaccharide (LPS)-binding protein in neutralization of LPS and enhancement of LPS-induced activation of mononuclear cells. Infect Immun 2001;69:6942–50.
[38] Gutsmann T, Haberer N, Seydel U, Wiese A. Interaction between lipopolysaccharides (LPS), LPS-binding protein (LBP), and planar membranes. Biol Chem 2001;382:425–34.
[39] Jack RS, Bernheiden M, Rune G, Ehlers M, Weber A, Kirsch G, et al. Lipopolysaccharide-binding protein is required to combat a murine Gram-negative bacterial infection. Nature 1997;389:742–5.
[40] Andrä J, Garidel P, Majerle A, Jerala R, Ridge R, Paus E, et al. Biophysical characterization of the interaction of *Limulus* polyphemus endotoxin neutralizing protein (ENP) with lipopolysaccharide. Eur J Biochem 2004;271:2037–46.
[41] Vallespi MG, Glaria LA, Reyes O, Garay HE, Ferrero J, Arana MJ. A *Limulus* antilipopolysaccharide factor-derived peptide exhibits a new immunological activity with potential applicability in infectious diseases. Clin Diagn Lab Immunol 2000;7:669–75.